Correlating Nickel Functionalities to Selectivity for Hydrogen Peroxide Electrosynthesis

*Miha Nosan,[1] Dušan Strmčnik,[2] Vasiliy Brusko,[3] Maria Kirsanova,[4] Matjaž Finšgar,[5] Ayrat M. Dimiev,[3] and Boštjan Genorio[1]**

[1]Faculty of Chemistry and Chemical Technology, University of Ljubljana, Večna pot 113, SI-1000 Ljubljana, Slovenia

[2]The National Institute of Chemistry, Hajdrihova ulica 19, SI-1000 Ljubljana, Slovenia

[3]*Laboratory* of *Advanced Carbon Nanomaterials*, *Kazan Federal University*, Kremlyovskaya Street 18, *Kazan* 420008, Russian Federation

[4]Advanced Imaging Core Facility, Skolkovo Institute of Science and Technology, 121205 Moscow, Russian Federation

[5]Faculty of Chemistry and Chemical Engineering, University of Maribor, Smetanova ulica 17, SI-2000 Maribor, Slovenia

ELECTRONIC SUPPLEMENTARY INFORMATION

Corresponding Author

*E-mail: bostjan.genorio@fkkt.uni-lj.si

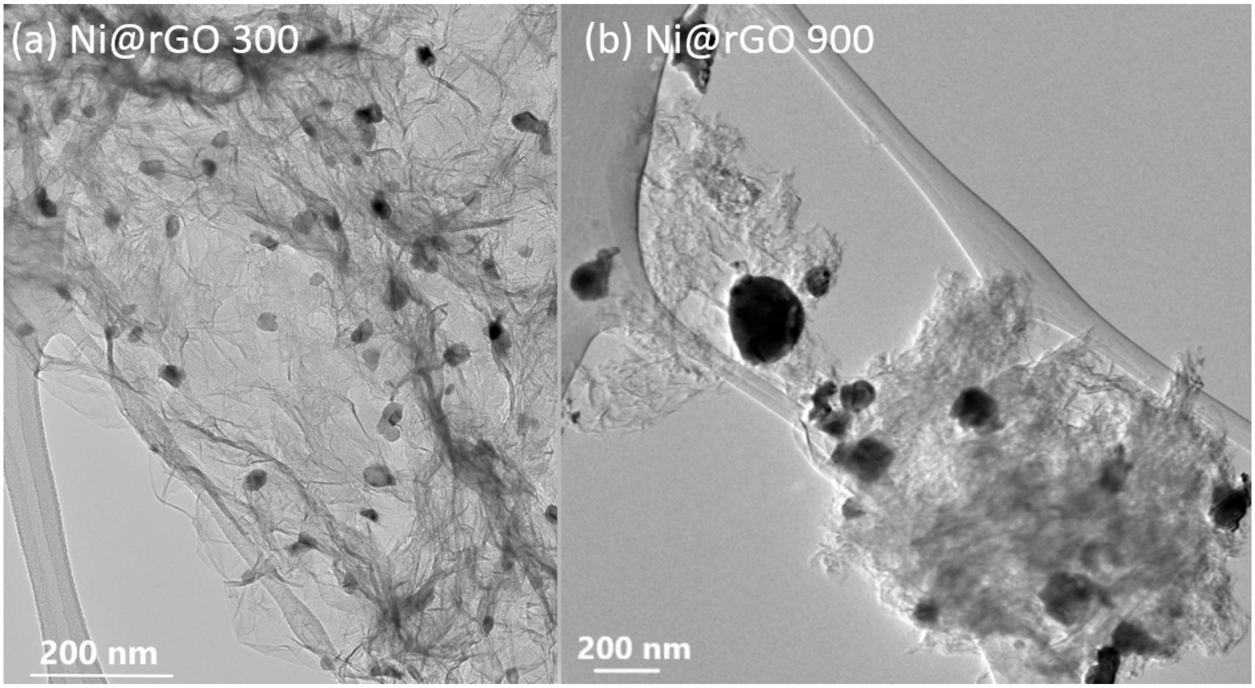

Figure S1: The TEM images of a) Ni@rGO 300 and b) Ni@rGO 900.

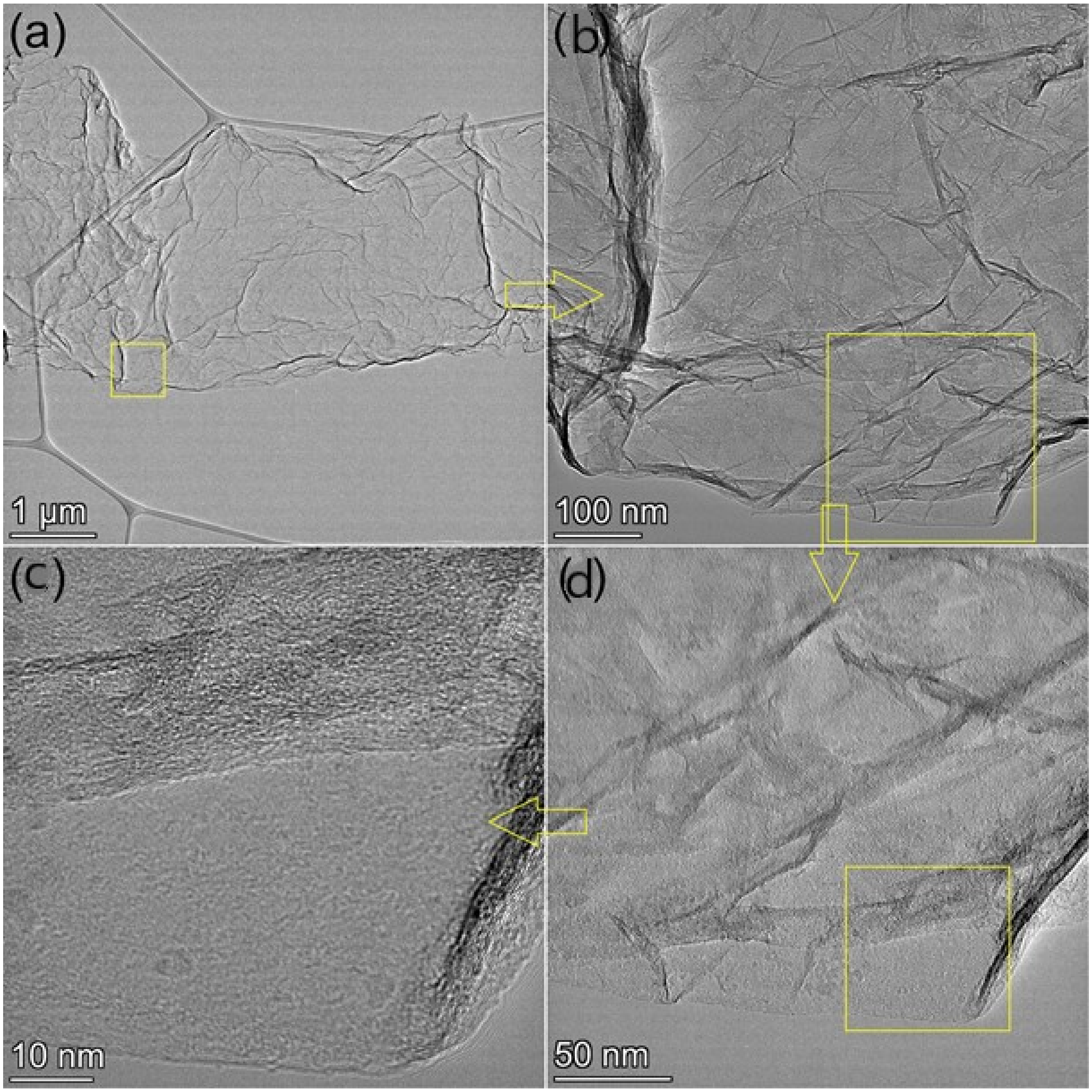

Figure S2: TEM images at different magnifications of Ni@rGO material.

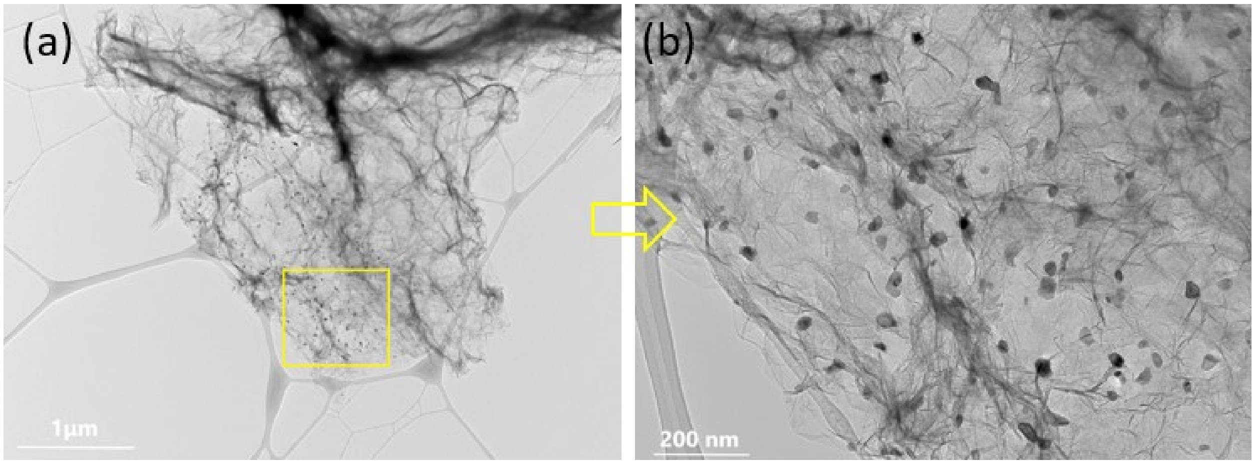

Figure S3: TEM images at different magnifications of Ni@rGO 300 material.

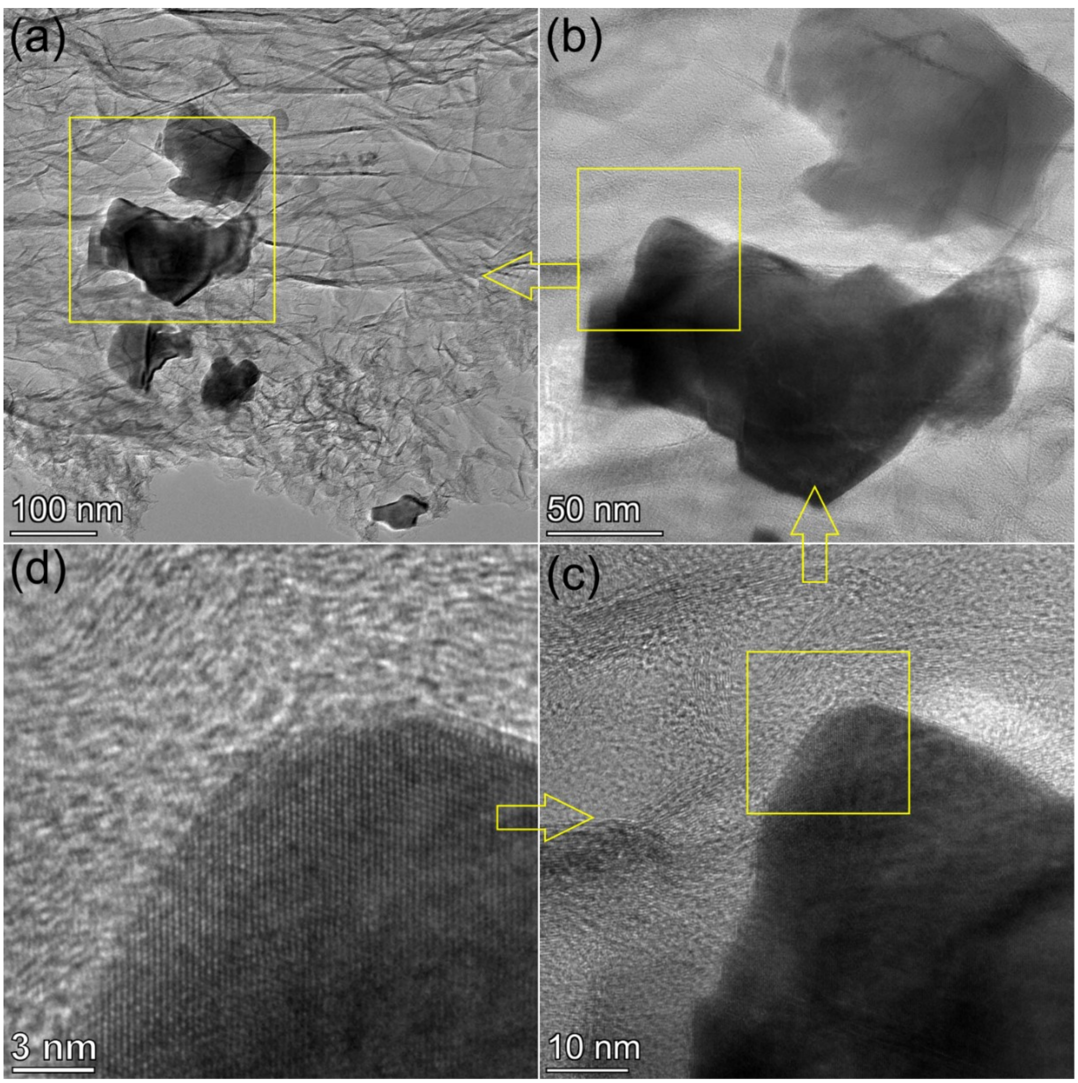

Figure S4: TEM images at different magnifications of Ni@rGO 900 material.

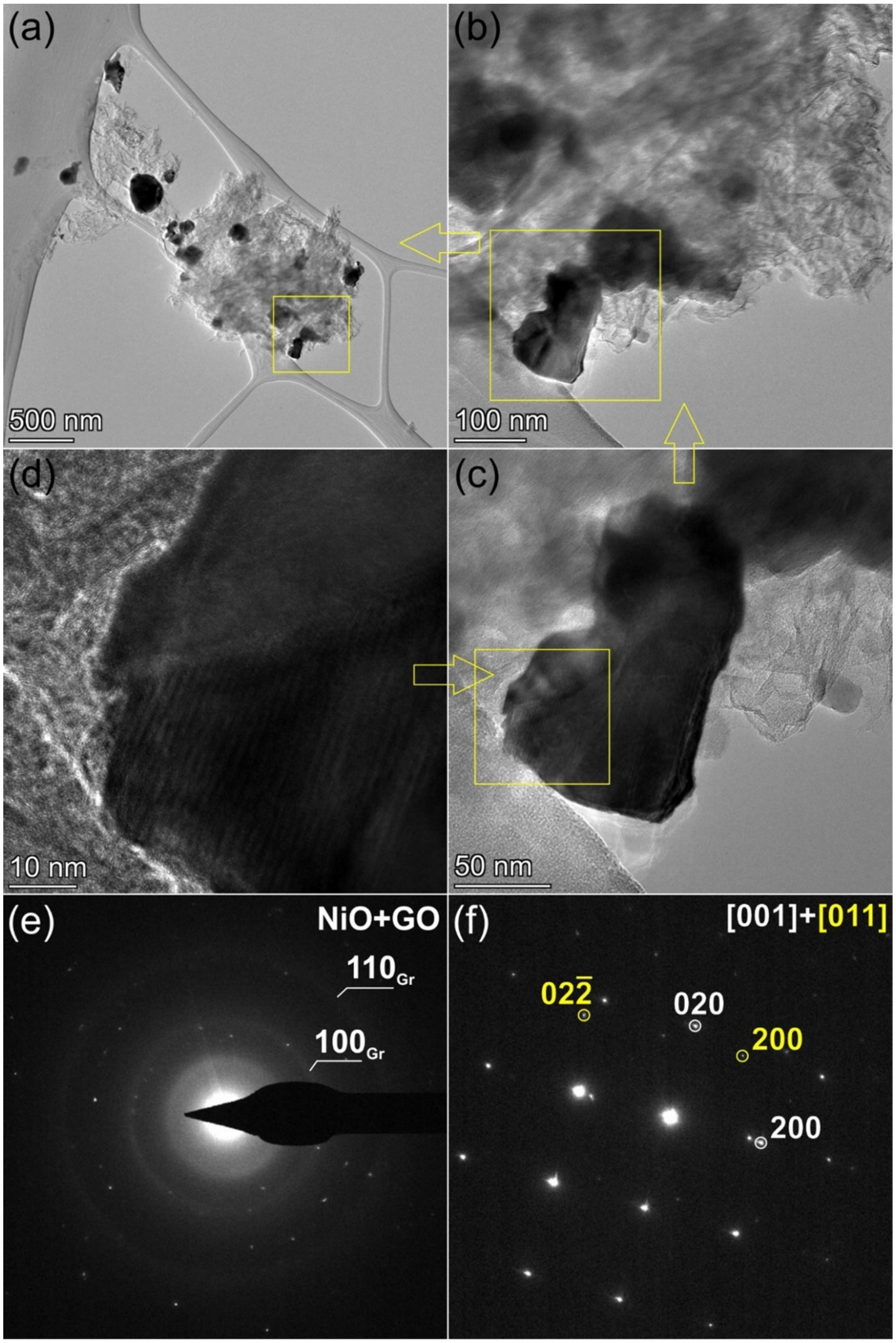

Figure S5: (a-d) A series of bright-field TEM images of Ni@rGO 900 material taken at different magnifications. (e) The electron diffraction, obtained from the entire region shown on (a). (f) The electron diffraction from an individual nanoparticle. The ED image (f) is indexed in the NiO cubic lattice.

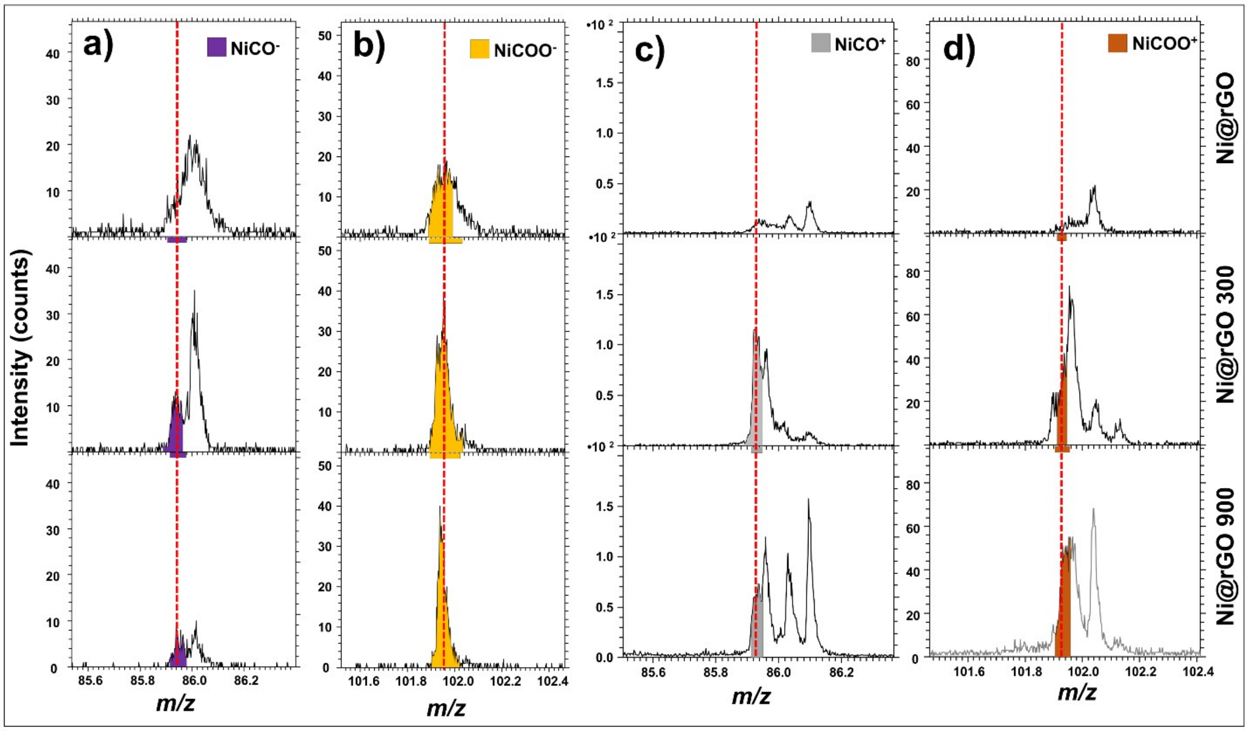

Figure S6: ToF-SIMS spectra of a) $NiCOO^-$, b) $NiCO^-$, measured in a negative polarity and c) $NiCOO^+$, d) $NiCO^+$, measured in a positive polarity for the Ni@rGO (upper), Ni@rGO 300 (middle) and Ni@rGO 900 (lower)

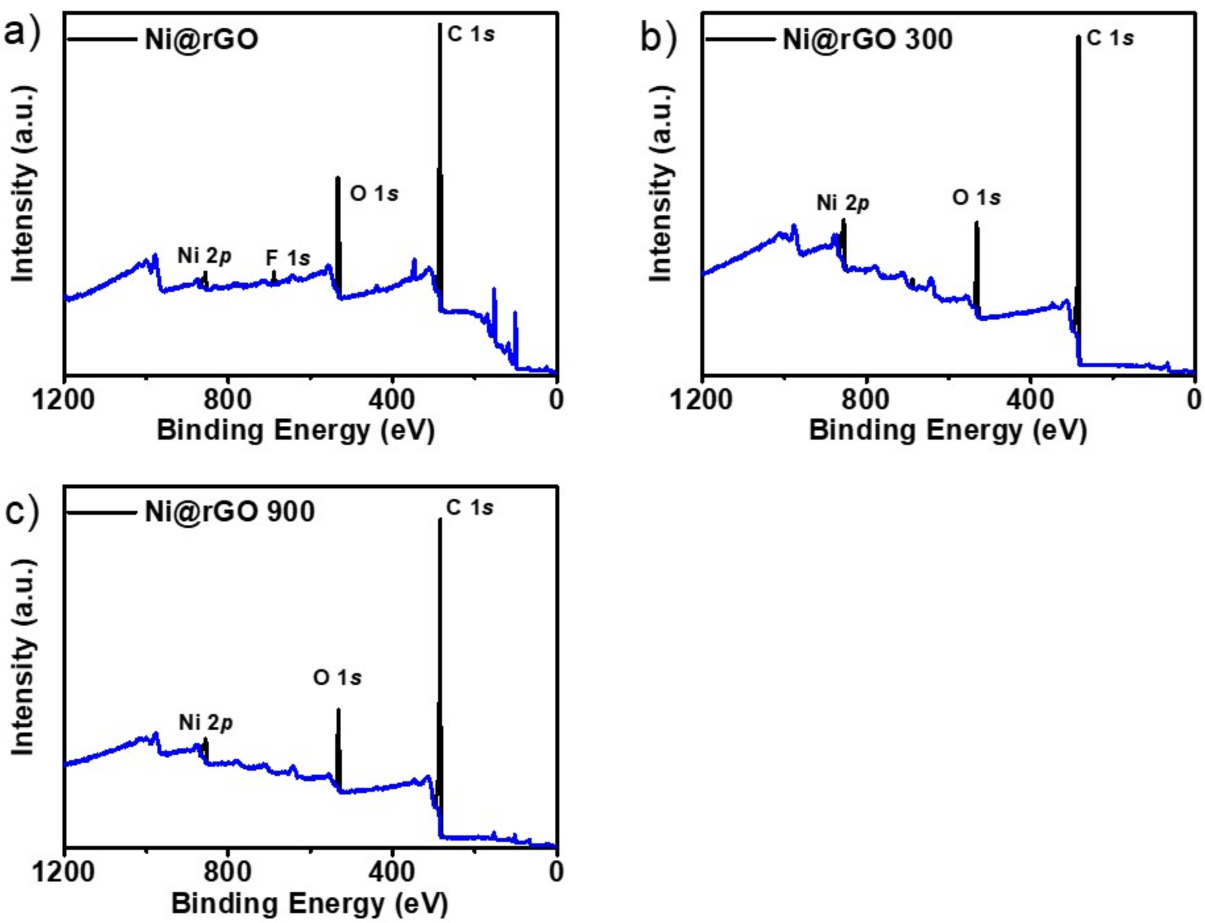

Figure S7: XPS survey spectra of a) Ni@rGO, b) Ni@rGO 300 and c) Ni@rGO 900 materials.

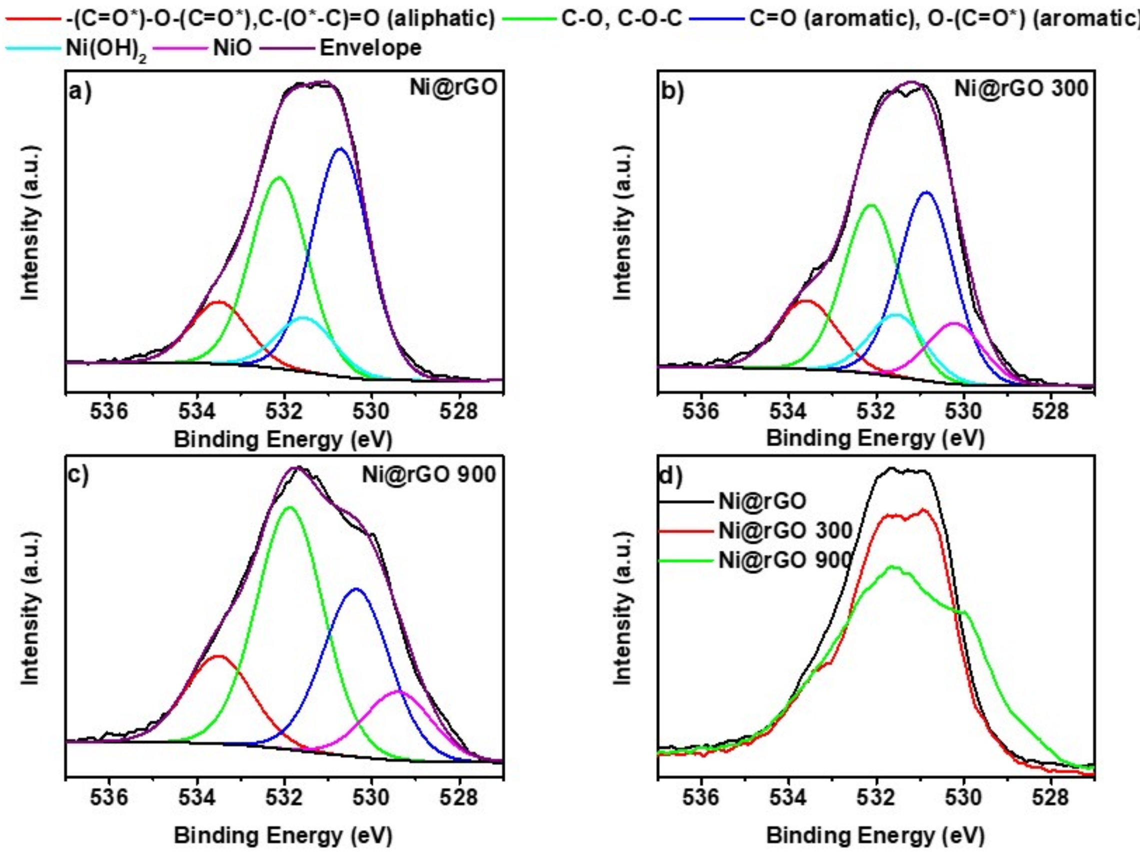

Name	-(C=O*)-O-(C=O*), O*-(C=O)-C	C-O, C-O-C	C=O O-(C=O*)-C	$Ni(OH)_2$	NiO
Ni@rGO	11.6	35.7	42.6	10.1	0.0
Ni@rGO 300	13.4	30.4	34.0	11.2	11.0
Ni@rGO 900	15.5	42.8	29.6	0.0	12.1

Figure S8: a) High-resolution O 1*s* XPS fitting of a) Ni@rGO, b) Ni@rGO 300, c) Ni@rGO 900 and d) the O 1*s* peak overlay.

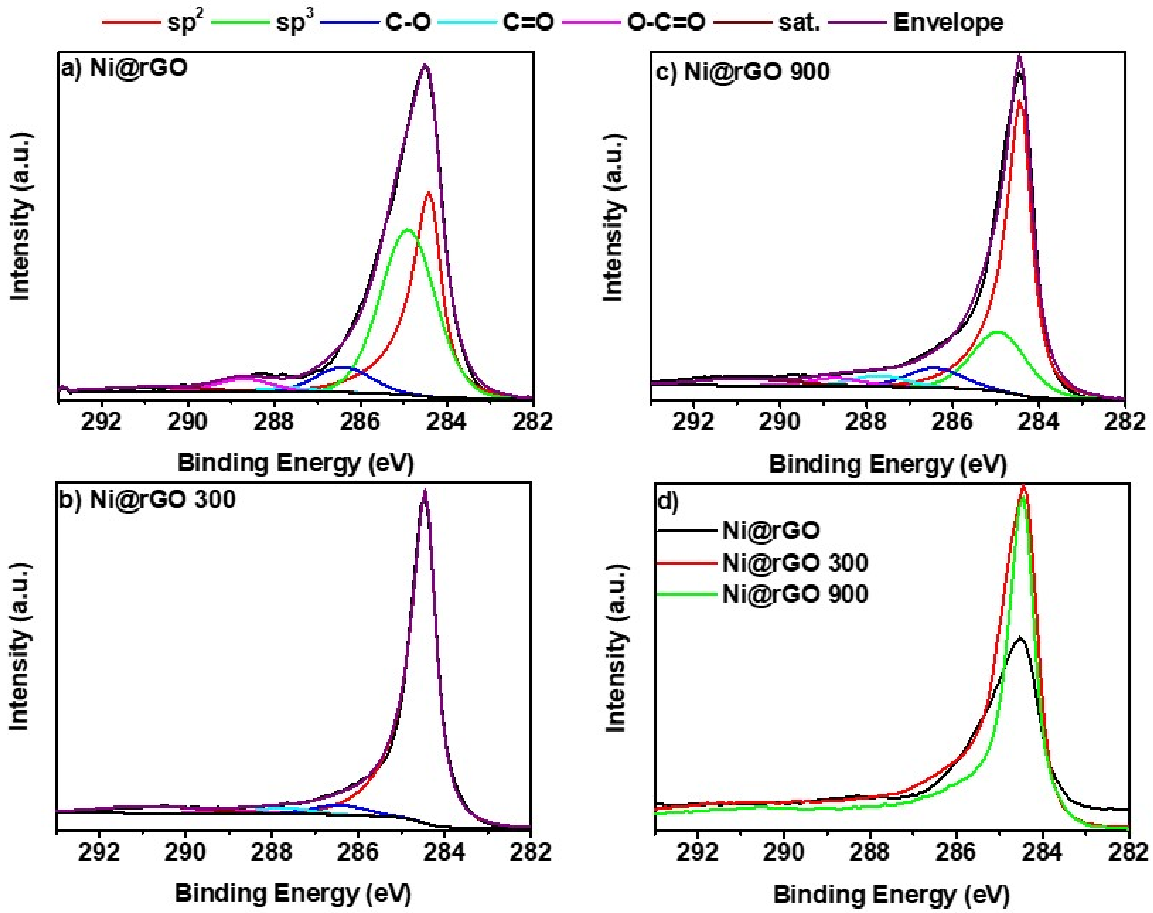

Name	*sp₂*	*sp₃*	C-O	C=O	O-C=O	sat.
Ni@rGO	39.8	45.7	6.9	1.2	3.6	2.8
Ni@rGO 300	62.5	20.0	6.6	3.7	2.8	4.4
Ni@rGO 900	86.1	0.0	4.1	2.6	1.2	6.0

Figure S9: a) High-resolution C 1*s* XPS fitting of a) Ni@rGO, b) Ni@rGO 300, c) Ni@rGO 900 and d) the C 1*s* peak overlay.

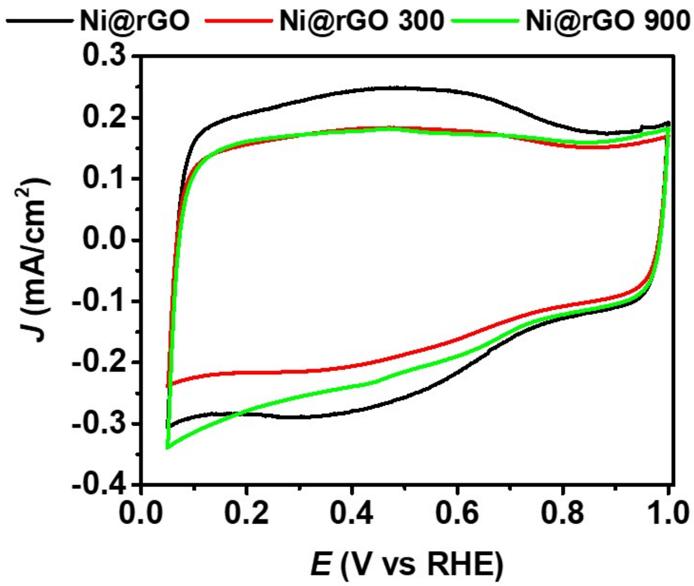

Figure S10: The CV of Ni@rGO (black), Ni@rGO 300 (red) and Ni@rGO (green) performed in Ar saturated 0.1 M KOH solution at a scan rate of 20 mV and 1600 rpm rotation speed.

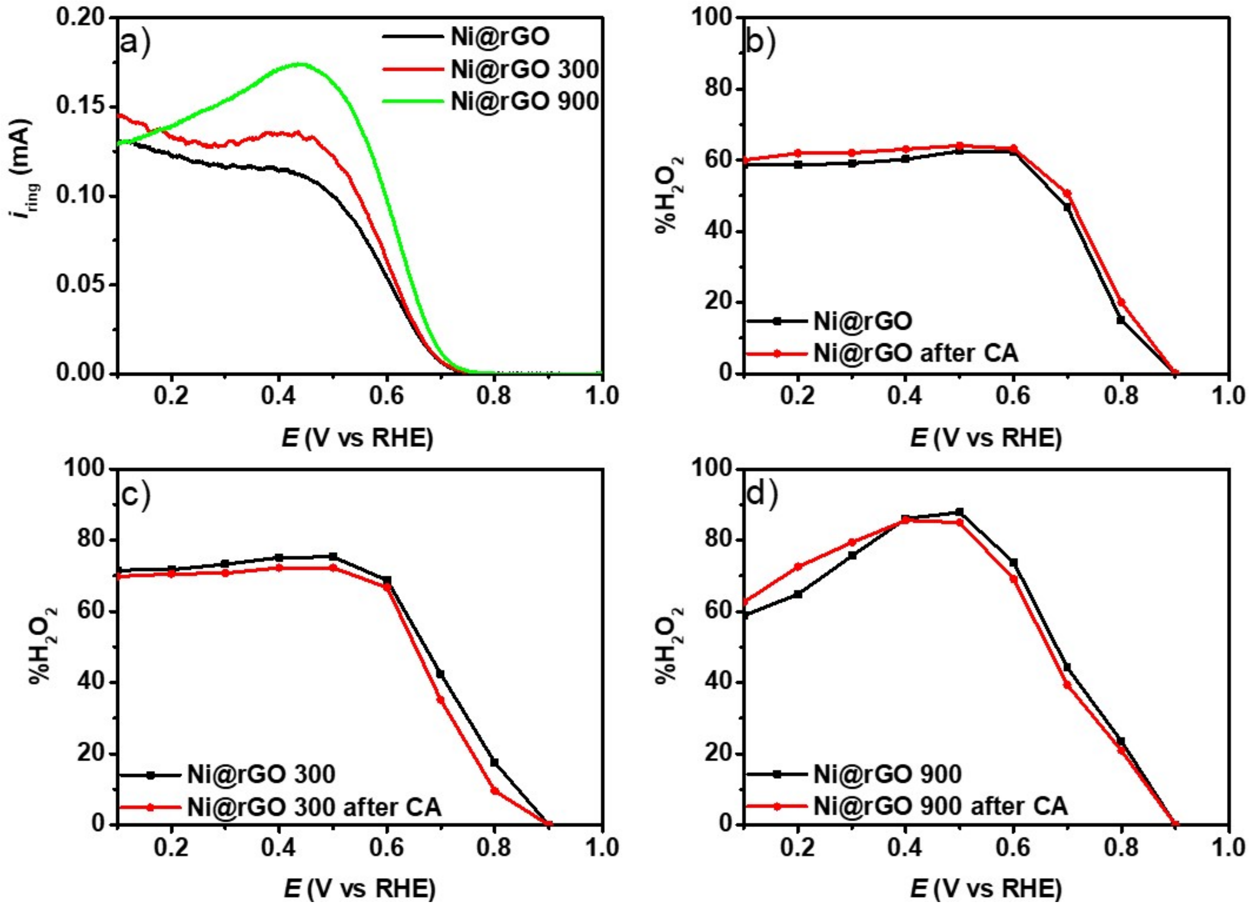

Figure S11: a) Current on the ring part of RRDE (at constant E = 1.3 V vs RHE) during the ORR selectivity study and the selectivity after the two-hour CA stability measurement for b) Ni@rGO c) Ni@rGO 300 and d) Ni@rGO 900 (green) in O_2 saturated 0.1 M KOH.

Table S1: Fitting parameters (binding energy, FWHM, peak area) for Ni $2p^{3/2}$ spectra.[1,2,3,4]

Parameters	**A**	**B**	**C**	**D**	**E**	**F**	**G**
Peak Name	Ni Metal^{1}	Ni Metal^{2}	Ni Metal^{3}	NiO^{1}	NiO^{2}	NiO^{3}	NiO^{4}
Peak Energy (eV)	852.6	856.3	858.7	853.7	855.4	860.9	864.0
FWHM	1.2	2.9	2.9	1.2	3.5	4.0	2.2
Peak Area	A	0.08 · A	0.15 · A	0.32 · E	E	0.77 · E	0.08 · E
	L	**H**	**I**	**J**	**K**	**M**	**N**
Peak Name	NiO^{5}	Ni(OH)$_2^{1}$	Ni(OH)$_2^{2}$	Ni(OH)$_2^{3}$	Ni(OH)$_2^{4}$	Ni(OH)$_2^{5}$	Ni(OH)$_2^{6}$
Peak Energy (eV)	866.3	854.9	855.7	857.7	860.5	861.5	866.5
FWHM	2.8	1.4	2.5	1.8	1.3	4.9	3.2
Peak Area	0.09 · E	0.16 · I	I	0.07 · I	0.03 · I	0.86 · I	0.08 · I

Table S2: Fitting of Ni $2p^{3/2}$ XPS spectra for Ni@rGO, Ni@rGO 300, and Ni@rGO 900 samples.

Material	NiO^{1}	NiO^{2}	NiO^{3}	NiO^{4}	NiO^{5}	Ni(OH)$_2^{1}$	Ni(OH)$_2^{2}$	Ni(OH)$_2^{3}$	Ni(OH)$_2^{4}$	Ni(OH)$_2^{5}$	Ni(OH)$_2^{6}$
Ni@rGO	0.75	2.33	1.8	0.19	0.21	6.89	43.04	3.01	1.29	37.05	3.45
Ni@rGO 300	4.43	13.86	10.68	1.11	1.25	4.98	31.13	2.18	0.93	26.79	2.49
Ni@rGO 900	12.25	43.77	33.72	3.51	3.94	0	0	0	0	0	0

The values are represented are based on total %Ni on the sample surface.

Supplementary References

1 A. P. Grosvenor, M. C. Biesinger, R. S. C. Smart and N. S. McIntyre, *Surf. Sci.*, 2006, **600**, 1771–1779.

2 M. C. Biesinger, B. P. Payne, L. W. M. Lau, A. Gerson and R. S. C. Smart, *Surf. Interface Anal.*, 2009, **41**, 324–332.

3 M. C. Biesinger, B. P. Payne, A. P. Grosvenor, L. W. M. Lau, A. R. Gerson and R. S. C. Smart, *Appl. Surf. Sci.*, 2011, **257**, 2717–2730.

4 M. C. Biesinger, L. W. M. Lau, A. R. Gerson and R. S. C. Smart, *Phys. Chem. Chem. Phys.*, 2012, **14**, 2434–2442.